Informed spatial regularizations for fast fusion of astronomical images

Claire Guilloteau, Thomas Oberlin, Olivier Berné, Nicolas Dobigeon

INFORMED SPATIAL REGULARIZATIONS FOR FAST FUSION OF ASTRONOMICAL IMAGES

Claire Guilloteau [⋆,†]*, Thomas Oberlin* [‡]*, Olivier Berné* [†] *and Nicolas Dobigeon* [⋆]

[⋆] University of Toulouse, IRIT/INP-ENSEEIHT, Toulouse, France.
[†] University of Toulouse, IRAP, Toulouse, France.
[‡] University of Toulouse, ISAE-SUPAERO, Toulouse, France.

ABSTRACT

This paper introduces two informed spatial regularizations dedicated to multiband image fusion. The fusion process combines a multispectral image with high spatial resolution and a hyperspectral image with high spectral resolution, with the aim of recovering a full resolution data-cube. In this work, we propose two spatial regularizations that exploit the spatial information of the multispectral image. A weighted Sobolev regularization identifies the sharp structures locations to locally mitigate a smoothness-promoting Sobolev regularization. A dictionary-based regularization takes advantage of spatial redundancy to recover spatial textures using a dictionary learned on the multispectral image. The proposed regularizations are evaluated on realistic simulations of James Webb Space Telescope (JWST) observations of the Orion Bar and show a better reconstruction of sharp structures compared to a non-informed regularization. Since JWST is now in orbit, we expect to use this method on real data in the near future.

***Index Terms*—** Data fusion, informed regularization, hyperspectral imaging, high dimensional imaging, astronomy.

1. INTRODUCTION

Hyperspectral (HS) imaging provides a full description of the acquired scene at high spectral resolution and has become, in the past two decades, a common technique for numerous spectral analyses, finding applications in remote sensing [1], planetology [2], material science [3], etc. This work focuses on astronomical HS imaging, particularly relevant to study key mechanisms of the interstellar medium or in cosmology. Observation instruments usually do not acquire spectro-images combining full spatial *and* spectral resolutions. Alternatively, astronomers typically observe the same scene with two complementary instruments providing an HS image with high spectral resolution and a multispectral (MS) image with high spatial resolution, respectively. The objective of the fusion task is to merge these two observations to recover a data-cube with high spectral and spatial resolutions.

Data fusion has been primarily studied for Earth observation. The original heuristic methods tackles the so-called *pansharpening* problem, which consists in combining a MS or HS image with a panchromatic image, with component substitution [4]. The first methods designed to fuse MS and HS images rely on spectral unmixing paradigms and low-rank approximations [5, 6]. Inverse problems approaches emerged more recently and has been proven to be the most efficient methods to fuse Earth observation data [7]. These methods exploit observation models to formulate an inverse problem complemented by spatial and spectral regularizations [8, 9].

Guided by these outcomes, we proposed in a previous work a MS/HS image fusion method dedicated to astronomical images [10]. We formulated an inverse problem derived from observation forward models, taking into consideration astronomical imaging specificities, namely the high dimensionality of the data and the spectrally variant blurs. This method relies on a low-rank approximation of the HS image and regularizes the problem via a Sobolev penalty that promotes smooth content. Under these assumptions, the resulting objective function can be efficiently minimized in a low-dimensional subspace after reformulating the problem in the Fourier domain. However, numerous astronomical scenes contain contrasting areas and sharp structures, e.g. fronts and/or small details, that can be poorly restored with a Sobolev regularized fusion process [11]. To overcome this limitation, this work shows that the spatial information brought by the high spatial resolution MS image can be conveniently and easily exploited to design quadratic informed spatial regularizations. These regularizations have the great advantage of preserving sharp structures identified in the MS image while preserving the computational efficiency of the fusion algorithm.

The paper is organized as follows. Section 2 introduces the fusion inverse problem derived from observational forward models. Section 3 describes the proposed informed spatial regularizations. We compare the performance of several spatial regularizations by fusing a realistic simulated dataset of the Orion Bar in Section 4. Section 5 concludes the paper.

Part of this work has been supported by the French National Research Agency under grant agreements ANR-19-PI3A-0004 (ANITI) and ANR-21-CE29-0007 (Imagin), the French Programme Physique et Chimie du Milieu Interstellaire (PCMI) funded by the Conseil National de la Recherche Scientifique (CNRS) and Centre National d'Études Spatiales (CNES).

2. PROBLEM STATEMENT

The observed MS and HS images are denoted by $\mathbf{Y}_{\mathrm{m}} \in \mathbb{R}^{l_{\mathrm{m}} \times p_{\mathrm{m}}}$ and $\mathbf{Y}_{\mathrm{h}} \in \mathbb{R}^{l_{\mathrm{h}} \times p_{\mathrm{h}}}$, respectively, where $l.$ and $p.$ refer to the numbers of spectral bands and pixels, with $l_{\mathrm{m}} \leq l_{\mathrm{h}}$ and $p_{\mathrm{h}} \leq p_{\mathrm{m}}$. They are assumed to be obtained through spectral and spatial degradations of a unobserved high resolution data-cube $\mathbf{X} \in \mathbb{R}^{l_{\mathrm{h}} \times p_{\mathrm{m}}}$

$$\mathbf{Y}_{\mathrm{m}} \approx \mathbf{L}_{\mathrm{m}} \mathcal{M}(\mathbf{X}) \tag{1}$$

$$\mathbf{Y}_{\mathrm{h}} \approx \mathbf{L}_{\mathrm{h}} \mathcal{H}(\mathbf{X}) \mathbf{S} \tag{2}$$

The spectral degradation operators $\mathbf{L}_{\mathrm{m}} \in \mathbb{R}^{l_{\mathrm{m}} \times l_{\mathrm{h}}}$ and $\mathbf{L}_{\mathrm{h}} \in \mathbb{R}^{l_{\mathrm{h}} \times l_{\mathrm{h}}}$ account for the spectral response of each instrument. The spatial degradation operators $\mathcal{M} : \mathbb{R}^{l_{\mathrm{h}} \times p_{\mathrm{m}}} \to \mathbb{R}^{l_{\mathrm{h}} \times p_{\mathrm{m}}}$ in (1) and $\mathcal{H} : \mathbb{R}^{l_{\mathrm{h}} \times p_{\mathrm{m}}} \to \mathbb{R}^{l_{\mathrm{h}} \times p_{\mathrm{m}}}$ in (2) are 2D spatial convolutions with spectrally variant kernels and model the blurs caused by the optical systems. This blur scales linearly with the wavelength, following the Rayleigh criterion [12]. The matrix $\mathbf{S} \in \mathbb{R}^{p_{\mathrm{m}} \times p_{\mathrm{h}}}$ stands for a 2D spatial downsampling operator with an integer decimation factor d such that $p_{\mathrm{h}} = \frac{p_{\mathrm{m}}}{d^2}$. Finally, the $\approx$ symbol models random noise and mismodeling. Recovering $\mathbf{X}$ from these two observations $\mathbf{Y}_{\mathrm{m}}$ and $\mathbf{Y}_{\mathrm{h}}$ can be formulated as a generic inverse problem

$$\hat{\mathbf{X}} = \underset{\mathbf{X}}{\operatorname{argmin}} \left(\frac{1}{2\sigma_{\mathrm{m}}^2} \|\mathbf{Y}_{\mathrm{m}} - \mathbf{L}_{\mathrm{m}} \mathcal{M}(\mathbf{X})\|_{\mathrm{F}}^2 + \frac{1}{2\sigma_{\mathrm{h}}^2} \|\mathbf{Y}_{\mathrm{h}} - \mathbf{L}_{\mathrm{h}} \mathcal{H}(\mathbf{X}) \mathbf{S}\|_{\mathrm{F}}^2 + \varphi_{\mathrm{spec}}(\mathbf{X}) + \varphi_{\mathrm{spac}}(\mathbf{X}) \right).$$

The two first terms refer to data fidelity terms and are related to the MS and HS forward models. The two additional terms $\varphi_{\mathrm{spec}}(\cdot)$ and $\varphi_{\mathrm{spec}}(\cdot)$ stand for spectral and spatial regularizations. As in previous works [5, 8, 10], the spectral regularization $\varphi_{\mathrm{spec}}(\cdot)$ is chosen to reflect the fact that the spectra in $\mathbf{X}$ are expected to live in a subspace whose dimensions l_{sub} is much smaller than the spectral dimension l_{h}. This assumption can be formulated by imposing a low-rank structure on fused image, i.e., $\mathbf{X} = \mathbf{V}\mathbf{Z}$. The columns of $\mathbf{V} \in \mathbb{R}^{l_{\mathrm{h}} \times l_{\mathrm{sub}}}$ span the signal subspace and are generally estimated beforehand from the HS image, e.g. by a principal component analysis (PCA). The matrix $\mathbf{Z} \in \mathbb{R}^{l_{\mathrm{sub}} \times p_{\mathrm{m}}}$ gathers the representation coefficients associated with the projection of $\mathbf{X}$ onto this subspace. In our previous work [10], the spatial penalization $\varphi_{\mathrm{spat}}(\cdot)$ is chosen as a conventional Sobolev regularization, which showed poor performance for restoring sharp details. The next section proposes two alternatives which exploit the spatial information brought by the MS image while preserving the efficiency of the optimization procedure.

3. INFORMED REGULARIZATIONS

This section derives two informed spatial regularizations $\varphi_{\mathrm{spa}}(\cdot)$: a weighted Sobolev-like regularization and a quadratic counterpart of a regularization based on a sparse representation in a dictionary. These two regularizations are formulated in the spectral subspace, i.e., they are directly applied to the representation coefficients $\mathbf{Z}$. This is equivalent to a direct formulation in the image domain, provided the matrix $\mathbf{V}$ is orthonormal. It is worth noting that we intentionally limit ourselves to quadratic regularizations for the sake of computationally efficiency, which is needed here given the huge dimension of the data.

3.1. Weighted Sobolev regularization

The first proposed regularization is based on the assumption that the image is predominantly smooth but may contain some sharp details. Generalizing the Sobolev regularization already used in [10], we thus define

$$\varphi_{\mathrm{spac}}(\mathbf{Z}) = \mu \|\mathbf{W} \odot (\mathbf{Z}\mathbf{D})\|_{\mathrm{F}}^2 \tag{3}$$

where $\mathbf{D}$ is a 1^{st} order 2D finite differences operator, $\mathbf{W}$ is a weighting matrix, $\odot$ accounts for the term-wise product and $\mu \geq 0$ is the regularization parameter adjusting the strength of the regularization. In smooth regions, coefficients in $\mathbf{W}$ should be set to large values to promote smoothness whereas around sharp structures, coefficients should be set to smaller values. Following a empirical Bayesian approach, the weighting matrix $\mathbf{W}$ is computed from the observed MS image $\mathbf{Y}_{\mathrm{m}}$ of high resolution as follows

$$(\mathbf{W})_p = \left[\operatorname{diag} \left(\mathbf{V}^T \mathbf{V} \frac{\|(\mathbf{Y}_{\mathrm{m}} \mathbf{D})_p\|_F^2}{\operatorname{tr}(\mathbf{L}_{\mathrm{m}} \mathbf{L}_{\mathrm{m}}^T)} \right) + \epsilon \right]^{-1} \tag{4}$$

where p stands for the current pixel index and $\epsilon > 0$ is a small hyperparameter preventing denominator values to be zero. The main asset of this regularization is the use of the observed high spatial resolution information to mitigate the effect of a smoothness-promoting regularization, thus making it adaptable to a large range of astrophysical scenes.

3.2. Dictionary-based regularization

The second proposed informed regularization is inspired by the regularization proposed in [9] and adapted in this work for astronomical image fusion tasks. Using a hierarchical Bayesian approach and a Gaussian *prior*, the regularization is defined as

$$\varphi_{\mathrm{spat}}(\mathbf{Z}) = \mu \|\mathbf{Z} - \widetilde{\mathbf{Z}}\|_{\mathrm{F}}^2. \tag{5}$$

The authors in [9] define the prior mean $\widetilde{\mathbf{Z}}$ as a sparse linear combination of atoms from an overcomplete dictionary, i.e.

$$\widetilde{\mathbf{Z}} = \mathcal{P}(\mathbf{B}\mathbf{C})$$

where $\mathcal{P}(\cdot) : \mathbb{R}^{l_{\mathrm{sub}} p_{\mathrm{p}} \times n_{\mathrm{p}}} \to \mathbb{R}^{l_{\mathrm{sub}} p_{\mathrm{m}}}$ is a linear operator combining n_{p} overlapping patches. The overcomplete dictionary $\mathbf{B} \in \mathbb{R}^{l_{\mathrm{sub}} p_{\mathrm{p}} \times n_{\mathrm{a}}}$ is composed of n_{a} atoms and $\mathbf{C} \in \mathbb{R}^{n_{\mathrm{a}} \times n_{\mathrm{p}}}$ is the coding matrix. Thereafter, our method differs from the approach proposed in [9]. In the latter, the dictionary $\mathbf{B}$ and the support of coding coefficients are estimated on an approximation of the solution of the fusion problem. In this work,

the goal is to take maximum advantage of the high spatial resolution and high frequency information that is observed in the MS image and that could be lost in an approximation of the fused data-cube. Hence, we propose to identify the dictionary and the support of coding coefficients from the observed MS image. More precisely, the overcomplete dictionary $\mathbf{B}$ is first learned from MS image patches using online dictionary learning (ODL) [13]. As an output of this process, an estimate $\mathbf{C}_{\mathrm{m}}$ of a coding matrix for all MS bands is provided. This coding matrix is then re-estimated using orthogonal matching pursuit (OMP). A first estimation of the coding matrix $\mathbf{C}$ is obtained by averaging $\mathbf{C}_{\mathrm{m}}$ over the MS bands. The support of this matrix is then defined by the non-zero entries of $\mathbf{C}$. The atoms of the dictionary $\mathbf{B}$ possibly activated to form each patch are thereby identified during this step and extracted from the observed high spatial resolution MS image.

3.3. Fast implementation

Although quadratic, the optimization problem introduced in Section 2 cannot be easily solved by conventional methods as fast gradient descent [14] or conjugate gradient [15] due to spectrally variant blur operators in each forward models. Indeed, storing and processing a few thousands of distinct PSFs annihilate the dimension reduction induced by the spectral regularization. However, we proposed in [10] to handle convolutions as well as the high dimensionality of the data by solving the problem in the frequency domain and in the low-dimensional spectral subspace when using a non-informed Sobolev spatial regularization. The strategy is adapted here to solve the fusion inverse problem complemented with the informed regularizations described in Sections 3.1 and 3.2.

The weighted Sobolev regularization in Eq. (3) includes a term-wise product between $\mathbf{W}$ and $\mathbf{ZD}$ that cannot be wisely expressed in the Fourier domain. Nevertheless, this regularization is defined in the low-dimensional spectral subspace and does not involve the projection operator $\mathbf{V}$. This weighted Sobolev regularized inverse problem can thus be solved efficiently following the strategy in [10] performing direct and inverse Fourier transforms to compute the term-wise products in the image domain but in a low-dimensional spectral subspace, at low cost.

The dictionary-based regularized fusion problem is an optimization problem with respect to two variables $\mathbf{Z}$ and $\mathbf{C}$. The approach proposed in [9] and used here consists in solving the problem with a block coordinate descent algorithm, minimizing alternatively the objective function with respect to each variable, one at a time. First, the optimization task with respect to $\mathbf{Z}$ conditionally on $\mathbf{C}$ can be performed using the strategy proposed in [10] at reasonable computational cost. Secondly, the optimization problem with respect to $\mathbf{C}$ conditionally on $\mathbf{Z}$ is a least-square problem whose solution can be analytically and rapidly calculated at each iteration of the alternate optimization algorithm [9].

4. EXPERIMENTS

Synthetic data – The relevance of each proposed regularization is assessed within the fusion process performed on a realistic simulated dataset of the Orion Bar. This dataset is composed of a high resolution synthetic reference image of the Orion Bar and corresponding HS and MS images [11]. It has been generated to asses high dimensional astronomical data fusion. The reference scene is composed of 90×900 pixels and 4974 spectral bands from 1 to 2.35 microns, in the near-infrared range. The reference image is shown in Fig. 1 as a RGB composition of 3 spectral bands.

From this reference scene and following forward models (1) and (2), MS and HS images have been computed as they would be observed by the near-infrared camera (NIRCam) imager and the near-infrared spectrograph integral field unit (NIRSpec IFU) embedded in the James Webb Space Telescope [11]. These images correspond to observations which have been planned as part of the PDRs4All observing program [16], and will be obtained in 2022. The MS image is made of 11 spectral bands and 90×900 pixels and the HS image is composed of 4974 spectral bands and 30×300 pixels such that the subsampling factor $d = 3$. The degradation operators involved in forward models are provided by JWST documentation [17, 18, 19], including a mixed Poisson-Gaussian noise. RGB compositions of 3 spectral bandx of HS and MS images are shown in Fig 1.

Compared methods – Hereafter, we compare high dimensional fusion methods complemented with the two informed regularizations proposed in Section 3 and complemented with a conventional (i.e., non-informed) Sobolev regularization. The latter is proposed in [10] and has been shown to outperform state-of-the-art methods for astronomical data fusion on this relatively smooth scene.

The subspace identification required by these methods has been performed in this work by a PCA on the HS image. The dictionary-based regularization involves a few hyperparameters. The number of atoms in the dictionary has been set to 64. Each patch has a pre-determined size of 9×9 pixels with a 6 pixels overlapping. The maximum number of atoms per patch is 6. Finally, in Eq. (5), $\epsilon \simeq 10$. These parameters have been chosen empirically to obtain the best quantitative results.

Results – Fig. 1 displays RGB compositions of fusion products obtained with the Sobolev, the weighted Sobolev and the dictionary-based regularization along with the ground-truth reference image and the MS and HS observed images. Zooms on sharp structures are shown in Fig. 2. Overall, the reconstruction appears to be visually excellent. Spectral contrast and most of spatial details are restored and denoising seems to be efficient for each method. Sharp structures, in light blue, come out slightly smoothed. However, the intensity of this front is better restored with the use of the weighted Sobolev

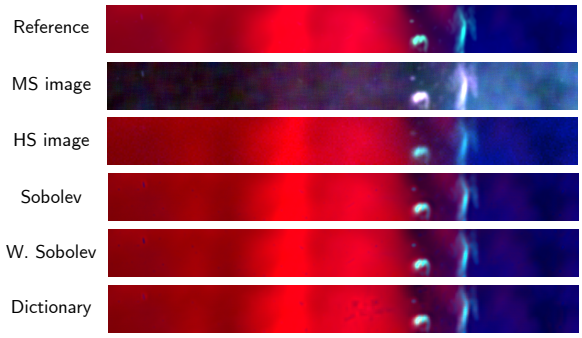

Fig. 1. RGB compositions of the reference image, the multispectral observed image, the hyperspectral observed image and fused products with the Sobolev, the weigthed Sobolev and the dictionary-based regularizations.

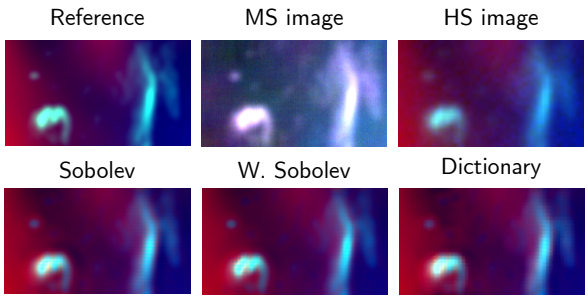

Fig. 2. Zooms on strong structures from Fig. 1.

regularization. On the contrary, these structures are less sharp in the fusion product obtained with the dictionary-based regularization. Moreover, the fused image shows a 9×9 pixels pattern due to patches and an artefact in the smooth region in red.

To quantitatively evaluate the reconstruction, we introduce three comprehensive metrics. The average spectral angle mapper (aSAM) [20] assesses the quality of the spectral reconstruction through the measure of the spectral distortion between reference and reconstructed spectra. The average complementary structural similarity index (acSSIM) [21] estimates the degradation of spatial structures on each spectral band thus evaluating the quality of the spatial reconstruction. Finally, the peak signal-to-noise ratio (PSNR) quantifies the overall quality reconstruction in the least-square sense. A good reconstruction is fulfilled with low values of aSAM and acSSIM and a large value a PSNR. Table 1 reports quantitative results calculated over the entire field-of-view shown in Fig. 1 while Table 2 shows metric values calculated on the sharp structures areas displayed in Fig. 2. On the full field-of-view, the spectral reconstruction metric is about 10% less good for the dictionary-based reconstructed image. The spatial reconstruction of the weigthed Sobolev fusion image is 10 to 15% better than the other reconstructed images.

Table 1. Performance of fusion methods : aSAM (rad), acSSIM, PSNR (dB), and time (preprocessing + fusion).

Methods	aSAM	acSSIM	PSNR	Time (s)
Sobolev	**0.025**	0.0022	73.75	**2200 + 15**
W. Sobolev	**0.025**	**0.0020**	**74.97**	2200 + 75
Dictionary	0.028	0.0024	73.01	2700 + 15

Table 2. Performance of fusion methods evaluated on sharp details areas : aSAM (rad), acSSIM et PSNR (dB).

Methods	aSAM	acSSIM	PSNR
Sobolev	0.053	0.0046	65.69
W. Sobolev	**0.051**	**0.0038**	**66.92**
Dictionary	0.064	0.0045	65.04

This method also improves by 1dB and by almost 2dB the global reconstruction of the fusion with the Sobolev and the dictionary-based regularizations, respectively. As expected, the use of the Sobolev regularization slightly speeds up the fusion task, as less computations are required. Evaluated only on the sharp structured area depicted in Fig. 2, the spectral, spatial and global reconstruction appears to be much better with the weighted Sobolev regularization. Note that the dictionary regularization is clearly outperformed by weighted Sobolev, because the scene is mostly smooth and does not contain much spatial redundancy. When it does and according to our experience on other simulations, the dictionary regularization can become quite competitive.

5. CONCLUSION

In this paper, we proposed two informed spatial regularizations to fuse high dimensional astronomical images. We formulated a weighted Sobolev and a dictionary-based regularizations whose parameters were derived from the high spatial resolution observations. These regularizations complemented a fusion inverse problem relying on observation forward models including astronomical instruments specificities such as spectrally variant blurs. The problem was solved efficiently exploiting a fast implementation derived from our previous work. We tested the proposed regularizations on a realistic simulated dataset of the Orion Bar and showed that the weighted Sobolev regularization outperformed a non-informed regularization to recover sharp spatial structures. Future work will be dedicated to perform extensive tests on real data from the James Webb Space Telescope which is currently in orbit.

6. REFERENCES

[1] C.-I Chang, *Hyperspectral Data Exploitation: theory and applications*. Hoboken, NJ: John Wiley & Sons, 2007.

[2] S. Douté, B. Schmitt, Y. Langevin, J.-P. Bibring, F. Altieri, G. Bellucci, B. Gondet, F. Poulet, and the MEX OMEGA team, "South Pole of Mars: Nature and composition of the icy terrains from Mars Express OMEGA observations," *Planetary and Space Science*, vol. 55, pp. 113–133, Jan 2007.

[3] C. Colliex, M. Tencé, E. Lefèvre, C. Mory, H. Gu, D. Bouchet, and C. Jeanguillaume, "Electron energy loss spectrometry mapping," *Microchimica Acta*, vol. 114, pp. 71–87, 1994.

[4] G. Vivone, L. Alparone, J. Chanussot, M. Dalla Mura, A. Garzelli, G. A. Licciardi, R. Restaino, and L. Wald, "A critical comparison among pansharpening algorithms," *IEEE Trans. Geosci. Remote Sens.*, vol. 53, no. 5, pp. 2565–2586, May 2015.

[5] O. Berné, A. Helens, P. Pilleri, and C. Joblin, "Non-negative matrix factorization pansharpening of hyperspectral data: An application to mid-infrared astronomy," in *Proc. IEEE GRSS Workshop Hyperspectral Image SIgnal Process.: Evolution in Remote Sens. (WHISPERS)*, 06 2010, pp. 1–4.

[6] N. Yokoya, T. Yairi, and A. Iwasaki, "Coupled Nonnegative Matrix Factorization Unmixing for Hyperspectral and Multispectral Data Fusion," *IEEE Trans. Geosci. Remote Sens.*, vol. 50, no. 2, pp. 528–537, Feb 2012.

[7] N. Yokoya, C. Grohnfeldt, and J. Chanussot, "Hyperspectral and multispectral data fusion : A comparative review of the recent literature," *IEEE Trans. Geosci. Remote Sens. Mag*, vol. 5, no. 2, pp. 29–56, Jun 2017.

[8] M. Simoes, J. Bioucas-Dias, L. B. Almeida, and J. Chanussot, "A Convex Formulation for Hyperspectral Image Superresolution via Subspace-Based Regularization," *IEEE Trans. Geosci. Remote Sens.*, vol. 53, no. 6, pp. 3373–3388, Jun 2015.

[9] Q. Wei, J. Bioucas-Dias, N. Dobigeon, and J.-Y. Tourneret, "Hyperspectral and multispectral image fusion based on a sparse representation," *IEEE Trans. Geosci. Remote Sens.*, vol. 53, no. 7, pp. 3658–3668, Jul 2015.

[10] C. Guilloteau, T. Oberlin, O. Berné, and N. Dobigeon, "Hyperspectral and multispectral image fusion under spectrally varying spatial blurs – application to high dimensional infrared astronomical imaging," *IEEE Trans. Comput. Imag.*, vol. 6, pp. 1362–1374, 2020.

[11] C. Guilloteau, T. Oberlin, O. Berné, É. Habart, and N. Dobigeon, "Simulated JWST datasets for multispectral and hyperspectral image fusion," *The Astronomical Journal*, vol. 160, no. 1, p. 28, Jun. 2020.

[12] L. Rayleigh, "Investigations in optics, with special reference to the spectroscope," *Monthly Notices of the Royal Astronomical Society : Letters*, vol. 40, p. 254, Feb 1880.

[13] J. Mairal, F. Bach, J. Ponce, and G. Sapiro, "Online dictionary learning for sparse coding," in *Proc. International Conference on Machine Learning (ICML)*, New York, NY, USA, 2009, p. 689–696.

[14] A. Beck and M. Teboulle, "A fast iterative shrinkage-thresholding algorithm for linear inverse problems," *SIAM J. Imag. Sci.*, vol. 2, pp. 183–202, 01 2009.

[15] J. R. Shewchuk, "An introduction to the conjugate gradient method without the agonizing pain," Carnegie Mellon University, Pittsburgh, PA, USA, Tech. Rep., 1994.

[16] O. Berné, É. Habart, E. Peeters, A. Abergel, E. A. Bergin, J. Bernard-Salas, E. Bron, J. Cami, S. Cazaux, E. Dartois *et al.*, "PDRs4All: A JWST early release science program on radiative feedback from massive stars," *arXiv preprint arXiv:2201.05112*, 2022.

[17] Space Telescope Science Institute (STScI), *NIRCam Filters, JWST User Documentation [Published 2017 November 29]*, Baltimore, MD, 2017. [Online]. Available: https://jwst-docs.stsci.edu/near-infrared-camera/nircam-instrumentation/nircam-filters

[18] ——, *NIRSpec DispeRemote Sens. Environmentrs and Filters, JWST User Documentation [Published 2017 March 29]*, Baltimore, MD, 2017. [Online]. Available: https://jwst-docs.stsci.edu/near-infrared-spectrograph/nirspec-instrumentation/nirspec-dispeRemote Sens. Environmentrs-and-filters

[19] ——, *NIRSpec Integral Field Unit, JWST User Documentation [Published 2017 March 29]*, Baltimore, MD, 2017. [Online]. Available: https://jwst-docs.stsci.edu/near-infrared-spectrograph/nirspec-instrumentation/nirspec-integral-field-unit

[20] F. A. Kruse, A. B. Lefkoff, J. W. Boardman, K. B. Heidebrecht, A. T. Shapiro, P. J. Barloon, and A. F. H. Goetz, "The spectral image processing system (SIPS) – interactive visualization and analysis of imaging spectrometer data," *Remote Sens. Environment*, vol. 44, no. 2-3, pp. 145–163, May 1993.

[21] Z. Wang, A. C. Bovik, H. R. Sheikh, and E. P. Simoncelli, "Image quality assessment: From error visibility to structural similarity," *IEEE Trans. Image Process.*, vol. 13, no. 4, pp. 600–612, Apr 2004.